ELSEVIER

Journal of Alloys and Compounds 330–332 (2002) 426–429

Journal of ALLOYS AND COMPOUNDS

www.elsevier.com/locate/jallcom

Electromigration of H vacancies in $YH_{3-\delta}$

S.J. van der Molen*, M.S. Welling, R. Griessen

Faculty of Sciences, Division of Physics and Astronomy, Vrije Universiteit, De Boelelaan 1081, 1081 HV Amsterdam, The Netherlands

Abstract

Electromigration of H vacancies in $YH_{3-\delta}$ is studied with the use of a simple optical technique. We analyze our results solving a linearized partial differential equation describing the process. Good agreement between experimental curves and analytical solutions is found. Our results imply that electromigration of H in this switchable mirror is dominated by a large wind force-like term.

Keywords: Hydrogen in metals; Switchable mirrors; Electromigration

1. Introduction

In 1996, Huiberts et al. discovered that the metal–insulator (MI) transition in thin yttrium and lanthanum films is accompanied by spectacular changes in their optical properties [1]. The virgin materials and their dihydrides are good metals, whereas the trihydrides are optically transparent insulators. So far, there is no consensus on the nature of the insulating ground state [2].

We focus on transport of H vacancies in $YH_{3-\delta}$ when an electric field **E** is present. The force $\mathbf{F} = Z^*e\mathbf{E}$ an impurity experiences, consists of two terms [3]. First, there is the 'direct' force $\mathbf{F}_d = Z_d e\mathbf{E}$. The magnitude of Z_d has been a source of discussion ever since it was claimed to be zero [3]. Second, there is the 'wind' force $\mathbf{F}_{wind} = Z_{wind}e\mathbf{E}$, due to a net momentum transfer to the impurity by scattering charge carriers. The theory of the wind force is well established in metallic systems: $Z_{wind} = K/\rho$, where ρ is the total resistivity and K is a constant. Experimentally, Z_d and Z_{wind} are found from the resistivity dependence of Z^* [4].

2. Experiment

Our samples are prepared by electron gun evaporation in ultra high vacuum. First, a 200-nm, polycrystalline Y layer is deposited on a sapphire substrate at 293 K (base pressure: $5 \cdot 10^{-9}$ mbar). Next, a narrow shadow mask is placed in front of the sample and a 30-nm Pd layer is evaporated. This results in two Pd strips covering the Y layer at both ends, leaving the middle part of the sample unprotected. This part is superficially oxidized in air, inhibiting local H_2 dissociation and recombination [5,6]. Therefore H can only enter the sample via the Pd cap layer where dissociation is catalyzed. For an experiment, the sample is mounted in a chamber equipped with optical windows, temperature control, and electrical leads. The chamber itself is placed onto the positioning table of an optical microscope (Olympus BX60F5), on top of which a 3-CCD camera is mounted, and 1 bar of H_2 gas is introduced. Using a method described elsewhere, we hydrogenate the film via the Pd strips to trihydride (see Fig. 1a) [7]. To study migration, some H is removed from the film, either by lowering the H_2 pressure (at constant temperature) or by increasing the temperature (at constant p_{H_2}), staying well above the $\beta - \gamma$ plateau (see Fig. 1b) [8,9]. Our experiment starts when the initial temperature and H_2 pressure are restored and the Pd-covered part of the film returns to its original H-concentration. However, there is still an area beneath the oxide cap containing extra vacancies (from now on, we focus on one side of the symmetric sample only). It serves as the initial distribution for lateral electromigration of H-vacancies. Since the optical transmission T_{opt} of an $YH_{3-\delta}$ film decreases when H is taken out, the vacancy-rich region is observed as a somewhat darker area (see Fig. 1c). This allows us to follow its evolution in the presence of an electric field. Although a large number of experiments were performed,

*Corresponding author.

E-mail address: sejan@nat.vu.nl (S.J. van der Molen).

0925-8388/02/$ – see front matter
PII: S0925-8388(01)01440-2

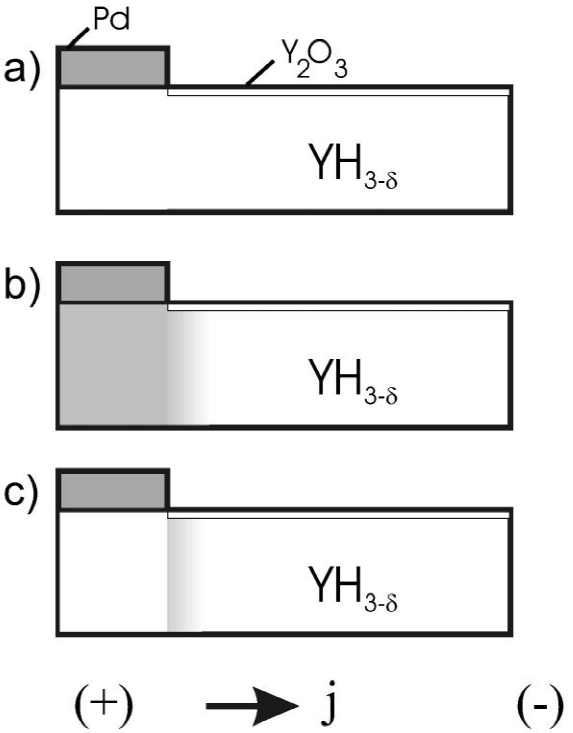

Fig. 1. Sample lay-out and experiment. Starting with an $YH_{3-\delta}$ sample (a), we take out some H via the Pd cap layer (b). Back in 1 bar H_2 and the desired temperature, only the Y beneath the Pd takes up H. The area just to the right of the Pd still contains H vacancies beneath an oxide skin and is detectable due to its lower optical transmission. In an electric field, the H vacancies migrate laterally. (Note that we focus on one half of the symmetric sample. Another Pd strip (not shown) is located to the right).

at temperatures between 292 and 408 K, we focus here on one representative experiment (see Ref. [10]).

3. Results and discussion

At $T = 343$ K, the evolution of the vacancy packet beneath the oxide cap is shown in the optical transmission photographs of Fig. 2 (current density $j = 2.5 \cdot 10^3$ A cm^{-2}). The vacancy distribution not only spreads out with time (a result of diffusion), but also moves with the electric field. From these photographs and the electrochemical data by Kooij et al. [9], we determine the *local* H concentration c. This yields the solid lines in Fig. 3. (Note that c is related to x in YH_x, Avogadro's number N_A and the hydrogen molar volume V_m by $c = x \cdot N_A / V_m$[1]).

For an analysis of our data, we use the theory of irreversible thermodynamics, in which the hydrogen flux J_H is described by $\mathbf{J}_H = -L_{HH}(\nabla\mu - Z^* e\mathbf{E})$, where μ is the chemical potential of H in $YH_{3-\delta}$. If $\mathbf{E} = 0$, this reduces to Fick's first law with the identification $D = L_{HH} \cdot \partial\mu/\partial c$. Using the continuity equation as well as $Z^* = Z_d + K/\rho$ and $E = \rho j$, we find:

$$\frac{\partial c}{\partial t} = \frac{\partial}{\partial z}\left[D\frac{\partial c}{\partial z} \right] - \frac{\partial}{\partial c}\left[\frac{D}{\partial\mu/\partial c}\left(Z_d + \frac{K}{\rho}\right) e\rho j \right] \frac{\partial c}{\partial z} \qquad (1)$$

As shown elsewhere, D is essentially concentration independent [10], allowing us to simplify Eq. (1):

$$\frac{\partial c}{\partial t} = D\frac{\partial^2 c}{\partial z^2} - v(c)\frac{\partial c}{\partial z} \qquad (2)$$

where z denotes the lateral distance to the Pd strip edge and

$$v(c) \equiv Dej \cdot \frac{\partial}{\partial c}\left[(\rho Z_d + K) \cdot (\partial\mu/\partial c)^{-1} \right] \qquad (3)$$

represents a translation velocity.

We demonstrate now that despite the apparent nonlinearity of $v(c)$, the evolution of the H distribution is well described by Eq. (2) using a constant v. For this we solve Eq. (2) with the following boundary conditions (we use $\tilde{c}(z,t)$ to denote the solutions of Eq. (2) and $c(z,t)$ for the experimental curves):

1. $\tilde{c}(z = 0,t) = c_{max}$, due to the fact that the YH_x beneath the Pd strip (located at $z \le 0$) is continuously in equilibrium with 1 bar H_2. From the isotherms by Kooij et al., we determine $c_{max} = 2.82 \cdot N_A / V_m$
2. $\tilde{c}(z = \infty,t) = c_{max}$, assuming that the other Pd strip is located at $z = \infty$.

The choice of the initial distribution $\tilde{c}_0(z) \equiv \tilde{c}(z,t = 0)$ is not as straightforward. Due to the time $\Delta t \sim 1$ min. it takes to return from the lower H_2 pressure to $p_{H_2} = 1$ bar, the first experimental peak is determined at some $t \equiv \Delta t$ rather than at $t = 0$. In other words, the initial vacancy distribution is somewhat ill-defined. Therefore we choose a two-step approach. First we solve Eq. (2) analytically, assuming an initial distribution of the form $\tilde{c}_0(z) = c_{max} - c_p \exp(-z^2/\eta^2)$. Second, we determine c_p, η and Δt by

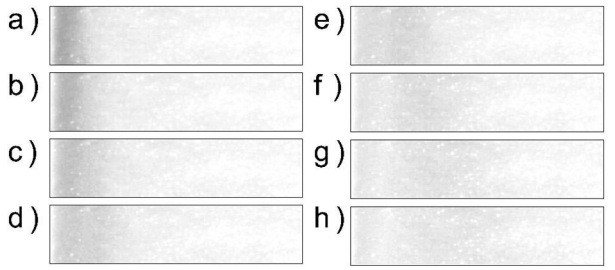

Fig. 2. Photographs in optical transmission of a typical vacancy electromigration experiment. The region of higher vacancy concentration (lower H concentration) in $YH_{3-\delta}$ is recognizable by its lower transmission ($T = 343$ K, $j = 2.5 \cdot 10^3$ A cm^{-2} from left (+) to right). The pictures are taken at (a): $t - \Delta t = 0$, (b): 62, (c): 155, (d): 279, (e): 527, (f): 1085, (g): 1705, (h): 2387 s. For clarity the contrast is enhanced, and the Pd covered part is not shown.

[1] As shown in Ref. [9], the molar volume is approximately concentration independent within the $YH_{3-\delta}$ phase.

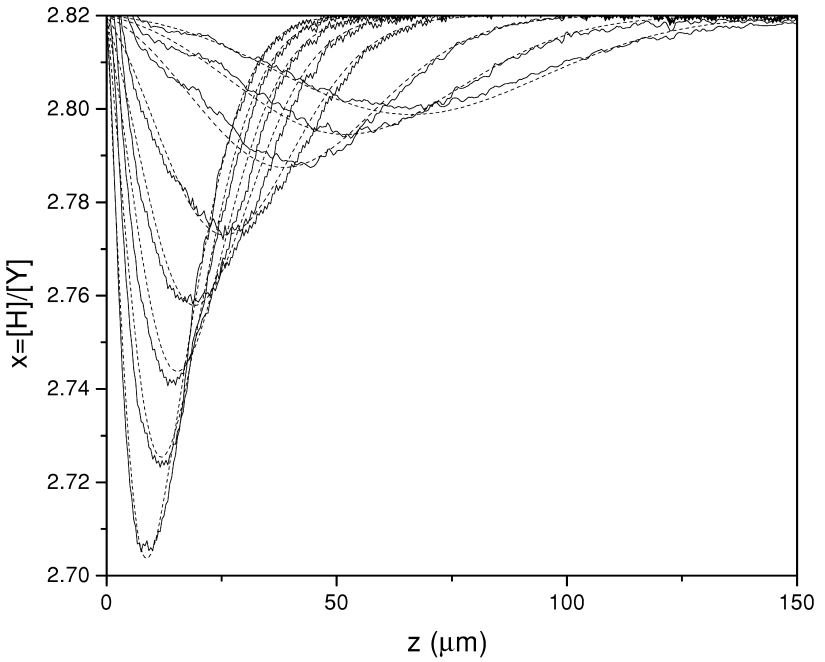

Fig. 3. Evolution of the local H-concentration. The experimental curves are calculated from the photographs in Fig. 2 (solid). The dashed curves are fits to the data based on Eq. (12), using constant parameters $D = 1.85 \cdot 10^{-9}$ cm^2 s^{-1} and $v = 19.5$ nm s^{-1}.

fitting the solution $\tilde{c}(z,t = \Delta t)$ to the first experimental peak $c(z,t = t_0 \equiv \Delta t)$.

To solve Eq. (2), we make two transformations: (i) $\tilde{\Delta}(z,t) = [c_{\max} - c(z,t)] \cdot V_M / N_A$ and (ii) $\tilde{\varepsilon}(z,t) = \tilde{\Delta}(z,t) \cdot \exp(-z \cdot v/2D)$, to arrive at

$$\frac{\partial \tilde{\varepsilon}}{\partial t} = D\frac{\partial^2 \tilde{\varepsilon}}{\partial z^2} - \frac{v^2}{4D}\tilde{\varepsilon} \tag{4}$$

The boundary conditions transform to $\tilde{\varepsilon}(z = 0,t) = 0$ and $\tilde{\varepsilon}(z = \infty,t) = 0$, whereas the initial distribution becomes $\tilde{\varepsilon}_0(z) = \tilde{\Delta}_0(z) \cdot \exp(-z \cdot v/2D)$. Separation of variables, i.e. $\tilde{\varepsilon}(z,t) = Z(z)T(t)$, yields

$$\frac{1}{T}\frac{\partial T}{\partial t} = \frac{1}{Z}\left(D\frac{\partial^2 Z}{\partial z^2} - \frac{v^2}{4D}Z\right) = -\lambda^2 \tag{5}$$

with λ eigenvalues. It immediately follows that $T = \exp(-\lambda^2 t)$. To solve for Z taking the boundary conditions into account, we assume $Z = \sin kz$, so that $\lambda^2 = Dk^2 + v^2/4D$. Putting T and Z back together, we can write $\tilde{\varepsilon}(z,t)$ as a sine-Fourier transform:

$$\tilde{\varepsilon}(z,t) = \int_0^\infty \mathrm{d}k \ \mathrm{e}^{-\frac{v^2}{4D}t - Dk^2 t} f(k) \sin kz \tag{6}$$

The function $f(k)$ is determined by the initial distribution $\tilde{\varepsilon}_0(z)$ through:

$$f(k) = \frac{2}{\pi}\int_0^\infty \mathrm{d}z \ \tilde{\varepsilon}_0(z) \sin kz \tag{7}$$

Transforming back to $\tilde{\Delta}(z,t)$, these relations become:

$$\tilde{\Delta}(z,t) = \mathrm{e}^{\frac{v}{2D}\left(z - \frac{v}{2}t\right)} \int_0^\infty \mathrm{d}k \ \mathrm{e}^{-Dk^2 t} f(k) \sin kz \tag{8}$$

and

$$f(k) = \frac{2}{\pi}\int_0^\infty \mathrm{d}z \ \tilde{\Delta}_0(z) \, \mathrm{e}^{-\frac{v}{2D}z} \sin kz \tag{9}$$

To insert the initial distribution, we use a two-step procedure. First we assume a delta function-shaped initial distribution around $z = z_c$, i.e. $\tilde{\Delta}_0(z) = \delta(z - z_c)$. Plugging this into Eq. (9), we find $f_\delta(k) = \frac{2}{\pi} \, \mathrm{e}^{-\frac{v}{2D}z_c} \sin kz_c$. Using $2 \sin\alpha \sin\beta = \cos(\alpha - \beta) - \cos(\alpha + \beta)$ and $\int_0^\infty \mathrm{d}z \ \mathrm{e}^{-a^2 z^2} \cos(bz) = \sqrt{\pi}/2a \cdot \exp(-b^2/4a^2)$ we arrive at:

$$\tilde{\Delta}_\delta(z,z_c,t) = \frac{1}{2\sqrt{\pi Dt}} \, \mathrm{e}^{-\frac{1}{4Dt}(z - z_c - vt)^2} \left(1 - \mathrm{e}^{-\frac{zz_c}{Dt}}\right) \tag{10}$$

The second step is to express the actual initial distribution as a superposition of delta functions using the identity $\tilde{\Delta}_0(z) = \int_0^\infty \mathrm{d}y \ \tilde{\Delta}_0(y)\delta(z - y)$. Because Eq. (4) is linear, the evolution of any initial distribution is described by a superposition of the evolution of delta functions [11], i.e

$$\tilde{\Delta}(z,t) = \int_0^\infty \mathrm{d}y \ \tilde{\Delta}_0(y)\tilde{\Delta}_\delta(z,y,t) \tag{11}$$

Integrating Eq. (11) with $\tilde{\Delta}_0(z) = \tilde{\Delta}_p \exp(-z^2/\eta^2)$ we find:

$$\tilde{\Delta}(\lambda,\tau) = \frac{0.5\Delta_p}{\sqrt{1+\tau}} \cdot \left[\exp\left(-\frac{(\lambda-\theta\tau)^2}{1+\tau} \right) \cdot \left\{ 1 + \mathrm{erf}\left(\frac{\lambda-\theta\tau}{\sqrt{\tau}\sqrt{1+\tau}} \right) \right\} - \exp\left(-\frac{(\lambda-\theta\tau)^2 + 4\theta\lambda}{1+\tau} \right) \cdot \left\{ 1 - \mathrm{erf}\left(\frac{\lambda-\theta\tau}{\sqrt{\tau}\sqrt{1+\tau}} \right) \right\} \right] \quad (12)$$

where the dimensionless variables τ, λ and θ are defined as $\tau \equiv 4Dt/\eta^2$, $\lambda \equiv z/\eta$ and $\theta \equiv v\eta/4D$, respectively. Transforming back to $\tilde{c}$ yields the desired solution.

The dashed curves in Fig. 3 represent the solutions $\tilde{c}(z,t)$ with $v = 19.5$ nm s^{-1} and $D = 1.85 \cdot 10^{-9}$ cm^2 s^{-1}. The values of c_p, η and Δt are determined by fitting the solution $\tilde{c}(z,t = \Delta t)$ to the first experimental peak $c(z,t = \Delta t)$. Unfortunately, one needs v and D for this (see Eq. (12)), so that c_p, η and Δt are not completely independent. However, it turns out that v and D are rather insensitive to small variations in c_p, η and Δt, and consequently c_p, η and Δt are nevertheless determined accurately. (Note that Δt is not really free as it is roughly locked by the experimental actions as mentioned above). We conclude that once the first curve has been fitted, all others are well described via Eq. (12) using only two, concentration independent parameters, v and D.

To discuss the physical implications of v being constant, we rewrite Eq. (3) as $v/Dej = Z_d\zeta(c) + K\gamma(c)$, defining $\zeta(x) \equiv \frac{\partial}{\partial c}[\rho(\partial\mu/\partial c)^{-1}]$ and $\gamma(x) \equiv \frac{\partial}{\partial c}[(\partial\mu/\partial c)^{-1}]$ (assuming Z_d and K are constant). In Ref. [10] we demonstrate that the second term dominates the first, implying that one is actually measuring K rather than Z^* in these experiments. Using the resistivity curves and isotherms measured by Kooij et al., we find $K \approx -60$ mΩ cm [9,10]. Compared to both experimental and theoretical work on the archetypical metal hydrides (PdH_x, NbH_x, VH_x), K is three orders of magnitude larger [4]. This suggests that the coupling between electron and hydrogen fluxes in $YH_{3-\delta}$, of which K is a measure through $J_H \approx -L_{HH}Kej$, cannot be described by the conventional theories of electromigration [10].

4. Conclusions

We study H vacancy migration in $YH_{3-\delta}$. The linearized partial differential equation describing the process is solved analytically, and its solutions give good agreement with the experiment. The fact that v and D are essentially constant, while $YH_{3-\delta}$ exhibits a metal–insulator transition, implies a wind force coefficient K that is orders of magnitude larger than in metallic metal hydride systems.

Acknowledgements

We thank W.H. Huisman, J.W.J. Kerssemakers, A.T.M. van Gogh, and E.S. Kooij for useful discussions and N.J. Koeman for the preparation of the samples. This work was supported by FOM, which is financed by NWO. We acknowledge financial contribution of the European Commission through the TMR program (research network 'Metal hydrides with switchable physical properties').

References

[1] J.N. Huiberts et al., Nature (London) 380 (1996) 231.
[2] P.J. Kelly, J.P. Dekker, R. Stumpf, Phys. Rev. Lett. 78 (7) (1997) 1315;
K.K. Ng et al., Phys. Rev. B 59 (8) (1999) 5398;
K.K. Ng et al., Phys. Rev. Lett. 78 (7) (1997) 1311;
R. Eder, H.F. Pen, G.A. Sawatzky, Phys. Rev. B 56 (1997) 10115;
P. van Gelderen et al., Phys. Rev. Lett. (in press);
T. Miyake et al., Phys. Rev. B 61 (24) (2000) 16491.
[3] R.S. Sorbello, Solid State Phys. 51 (1998) 159–231;
J. van Ek, A. Lodder, Defect Diff. Forum 1 (1994) 115–116;
A.H. Verbruggen, IBM J. Res. Develop. 32 (1988) 93.
[4] H. Wipf, in: G. Alefeld, J. Völkl) (Eds.), Hydrogen in Metals II, Topics Appl. Phys,, Vol. 29, Springer, Berlin, 1978, p. 273;
A.H. Verbruggen, R. Griessen, Phys. Rev. B 32 (2) (1985) 1426;
A.H. Verbruggen et al., J. Phys. F: Met. Phys. 16 (1986) 557;
R. Pietrzak, R. Szatanik, M. Szuszkiewicz, J. Alloys Comp. 282 (1999) 130.
[5] F.J.A. den Broeder et al., Nature (London) 394 (1998) 656;
M.C. Huisman, S.J. van der Molen, R.D. Vis, Nucl. Instr. Meth. B 158 (1999) 451;
A. Remhof et al., Phys. Rev. B 62 (3) (2000) 2164.
[6] S.J. van der Molen et al., J. Appl. Phys. 86 (11) (1999) 6107.
[7] S.J. van der Molen, W.H. Huisman, R. Griessen, J. Alloys Comp. 330–332 (2002) 430.
[8] M. Kremers et al., Phys. Rev. B 57 (8) (1998) 4943;
E.S. Kooij, A.T.M. van Gogh, R. Griessen, J. Electrochem. Soc. 146 (1999) 2990.
[9] E.S. Kooij et al., Phys. Rev. B 62 (15) (2000) 10088.
[10] S.J. van der Molen, M.S. Welling, R. Griessen, Phys. Rev. Lett. 85 (18) (2000) 3882.
[11] J. Crank, The Mathematics of Diffusion, Clarendon, Oxford, 1975.